

Measurement of the Lifetime and Separation Energy of 3H

Original

Measurement of the Lifetime and Separation Energy of 3H / Acharya, S., Adamová, D., Adler, A., Aglieri Rinella, G., Agnello, M., Agrawal, N., Ahammed, Z., Ahmad, S., Ahn, S.U., Ahuja, I., Akindinov, A., Al-Turany, M., Aleksandrov, D., Alessandro, B., Alfanda, H.M., Alfaro Molina, R., Ali, B., Ali, Y., Alici, A., Alizadehvandchali, N., et al.. - In: PHYSICAL REVIEW LETTERS. - ISSN 0031-9007. - ELETTRONICO. - 131:10(2023), pp. 1-13. [10.1103/physrevlett.131.102302]

Availability:

This version is available at: 11583/2990149 since: 2024-07-01T21:18:57Z

Publisher:

American Physical Society

Published

DOI:10.1103/physrevlett.131.102302

Terms of use:


This article is made available under terms and conditions as specified in the corresponding bibliographic description in the repository

Publisher copyright

(Article begins on next page)

Measurement of the Lifetime and Λ Separation Energy of ${}^3_{\Lambda}\text{H}$

S. Acharya *et al.**
(ALICE Collaboration)

 (Received 5 October 2022; revised 18 January 2023; accepted 21 July 2023;
published 5 September 2023; corrected 3 October 2023)

The most precise measurements to date of the ${}^3_{\Lambda}\text{H}$ lifetime τ and Λ separation energy B_{Λ} are obtained using the data sample of Pb-Pb collisions at $\sqrt{s_{\text{NN}}} = 5.02$ TeV collected by ALICE at the LHC. The ${}^3_{\Lambda}\text{H}$ is reconstructed via its charged two-body mesonic decay channel (${}^3_{\Lambda}\text{H} \rightarrow {}^3\text{He} + \pi^{-}$ and the charge-conjugate process). The measured values $\tau = [253 \pm 11(\text{stat}) \pm 6(\text{syst})]$ ps and $B_{\Lambda} = [102 \pm 63(\text{stat}) \pm 67(\text{syst})]$ keV are compatible with predictions from effective field theories and confirm that the ${}^3_{\Lambda}\text{H}$ structure is consistent with a weakly bound system.

DOI: [10.1103/PhysRevLett.131.102302](https://doi.org/10.1103/PhysRevLett.131.102302)

Hypernuclei are bound states of nucleons and hyperons that are particularly interesting because they can be used as experimental probes for the study of the hyperon-nucleon (Y-N) interaction. Searching for hypernuclei and exploring the Y-N interaction have been a source of fascination for nuclear physicists since the discovery of the first hypernuclei in 1953 [1]. In recent years, measurements of the hypertriton production and lifetime have stimulated an interesting debate in the high-energy physics community. The knowledge of the Y-N interaction has become more relevant recently due to its connection to the modeling of dense astrophysical objects like neutron stars [2,3]. Indeed, in the inner core of neutron stars the creation of hyperons is energetically favored compared to purely nucleonic matter [4]. The presence of hyperons as additional degrees of freedom leads to a considerable modification of the matter equation of state (EOS), prohibiting the formation of high-mass neutron stars. This is incompatible with the observation of neutron stars heavier than two solar masses [2,4], constituting what is referred to as the “hyperon puzzle.” Many attempts were made to solve this puzzle, e.g., by introducing three-body forces leading to an additional repulsion that can counterbalance the large gravitational pressure and allow for larger star masses [5,6]. To constrain the parameter space of such models, a detailed knowledge of the Y-N interaction and of the three-body Y-N-N interaction is mandatory, including Λ , Σ , and Ξ hyperons. Numerous particle correlation analyses [7,8] directly contribute to the determination of such interactions. In a complementary approach, the lifetime and the

binding energy of a hypernucleus reflect the strength of the Y-N interaction [9,10]. The current estimate of the separation energy of the Λ in the hypertriton is $B_{\Lambda} = 181 \pm 48$ keV [11], which results in a rms radius (average distance of the Λ to the deuteron) of the order of 10 fm [12–15]. Lower values (~ 90 keV) of B_{Λ} are favored when fitting the correlation functions for protons and Λ baryons [16–18], therefore new measurements are required to understand this tension. The latest theoretical calculations predict a different degree of dependence of the ${}^3_{\Lambda}\text{H}$ lifetime on its binding energy. For pionless effective field theory (EFT) [19] based calculations, the ${}^3_{\Lambda}\text{H}$ lifetime is very close to the free Λ lifetime, with very little binding energy dependence for B_{Λ} values spanning from 0 to 0.5 MeV. On the other hand, in the χ EFT approach [20], a stronger dependence on the binding energy is predicted for the ${}^3_{\Lambda}\text{H}$ lifetime being $\tau = (163 \pm 18)$ ps for $B_{\Lambda} = 410$ keV and $\tau = (234 \pm 27)$ ps for $B_{\Lambda} = 69$ keV. Previous measurements of the lifetime [21–26] and B_{Λ} [27] of ${}^3_{\Lambda}\text{H}$ in heavy-ion collisions have still quite large uncertainties. In this Letter, new measurements with unprecedented precision of the ${}^3_{\Lambda}\text{H}$ lifetime and binding energy are presented to address the questions about its structure.

The presented results are based on data collected during the 2018 Pb-Pb LHC run at a center-of-mass energy per nucleon pair of $\sqrt{s_{\text{NN}}} = 5.02$ TeV. The ALICE detector and its performance are described in detail in Refs. [28,29]. The data acquisition for Pb-Pb events is triggered by the V0A and V0C scintillation detectors [30], positioned at forward ($2.8 < \eta < 5.1$) and backward ($-3.7 < \eta < -1.7$) pseudorapidity, respectively. A coincidence of signals in both V0A and V0C is used as a minimum-bias trigger. In addition, two thresholds on the minimum amount of charge deposited on the V0 detector are employed to trigger on central and semicentral Pb-Pb collisions. A centrality estimator based on the V0 detector arrays [31] is used to select the 90% most central hadronic collisions. Events are further selected by allowing a 10 cm maximum displacement

*Full author list given at the end of the article.

Published by the American Physical Society under the terms of the [Creative Commons Attribution 4.0 International license](https://creativecommons.org/licenses/by/4.0/). Further distribution of this work must maintain attribution to the author(s) and the published article's title, journal citation, and DOI.

of the primary vertex along the beam axis from the nominal center of the experiment in order to benefit from the full acceptance of the detector. Finally, events with multiple reconstructed primary vertices are rejected to avoid ambiguous associations of ${}^3_{\Lambda}\text{H}$ candidates to their production vertices. In total, about 300 million events are selected for this analysis.

In Pb-Pb collisions at the LHC, approximately the same number of ${}^3_{\Lambda}\text{H}$ and ${}^3_{\Lambda}\bar{\text{H}}$ are expected to be produced. The ${}^3_{\Lambda}\text{H}$ decays are detected via the charged two-body channel ${}^3_{\Lambda}\text{H} \rightarrow {}^3\text{He} + \pi^-$ (and the corresponding charge-conjugated particles for ${}^3_{\Lambda}\bar{\text{H}}$). The decay products of the ${}^3_{\Lambda}\text{H}$ are tracked with the Inner Tracking System [32] and the Time Projection Chamber (TPC) [33], which are positioned within a solenoid providing a homogeneous magnetic field of 0.5 T in the direction of the beam axis. Charged particles are tracked over the full azimuth and in the pseudorapidity interval $|\eta| < 0.8$. The specific energy loss of the decay products of ${}^3_{\Lambda}\text{H}$ and ${}^3_{\Lambda}\bar{\text{H}}$ is also measured in the TPC, with a dE/dx resolution of about 5% [33,34]. The $n(\sigma_i^{\text{TPC}})$ variable represents the particle identification (PID) response in the TPC expressed in terms of the deviation between the measured and the expected dE/dx for a particle species i , in units of the detector resolution σ . The expected dE/dx is computed with a parametrized Bethe-Bloch function [29]. Pion and ${}^3\text{He}$ tracks within $\pm 5\sigma^{\text{TPC}}$ are selected.

The identified ${}^3\text{He}$ and π tracks are then used to reconstruct the ${}^3_{\Lambda}\text{H}$ weak-decay topology with an algorithm similar to the one employed in previous analyses [23,25,35]. By combining the information on the decay kinematics and decay vertex, several selection variables are defined. Those used in the analysis are the following: the distance of closest approach both from the primary and the decay vertex and the $n(\sigma_i^{\text{TPC}})$ of each daughter track; the number of clusters of the ${}^3\text{He}$ track in the TPC; the reconstructed p_T of the ${}^3_{\Lambda}\text{H}$;

and $\cos(\theta_p)$, where θ_p is the angle between the total momentum vector of the decay daughters and the straight line connecting the primary and secondary vertices. These variables are combined as a gradient-boosted decision tree classifier (BDT) [36,37] that is trained on a dedicated Monte Carlo (MC) simulated event sample. The MC sample consists of ${}^3_{\Lambda}\text{H}$ (decays) signals injected onto underlying Pb-Pb collisions simulated with the HIJING event generator [38]. The transverse momentum (p_T) distribution of the injected signals is given by the blast-wave [39] function, with parameters taken from simultaneous fits of the p_T distribution of light-flavored hadrons measured in Pb-Pb collisions [40]. Only candidates with $2 \leq p_T < 9 \text{ GeV}/c$ are considered. The particle transport through the detector material is done using GEANT4 [41], which simulates the interaction with the material and the weak decay of the ${}^3_{\Lambda}\text{H}$. The BDT is a supervised learning algorithm that determines how to discriminate between two or more classes, in this case signal and background, by examining sets of examples called the training sets. In this analysis, the training sets comprise ${}^3_{\Lambda}\text{H}$ signal candidates extracted from the MC sample and background candidates from paired like-sign ${}^3\text{He}$ and π tracks from data. For each ${}^3_{\Lambda}\text{H}$ candidate, the BDT combines topological and single-track variables to return a score, which is used to discriminate between signal or background. In particular, the most important variable employed by the BDT for the classification is the $\cos(\theta_p)$. Candidates with a BDT score higher than a given threshold are selected as signal. The threshold is defined to maximize the expected signal significance assuming a production yield as predicted by the thermal statistical hadronization model [13] for the ${}^3_{\Lambda}\text{H}$ and the background rate observed when combining like-sign ${}^3\text{He}$ and π pairs.

The ${}^3_{\Lambda}\text{H}$ lifetime is extracted by analyzing the proper decay length spectrum shown in Fig. 1. The sample of ${}^3_{\Lambda}\bar{\text{H}}$

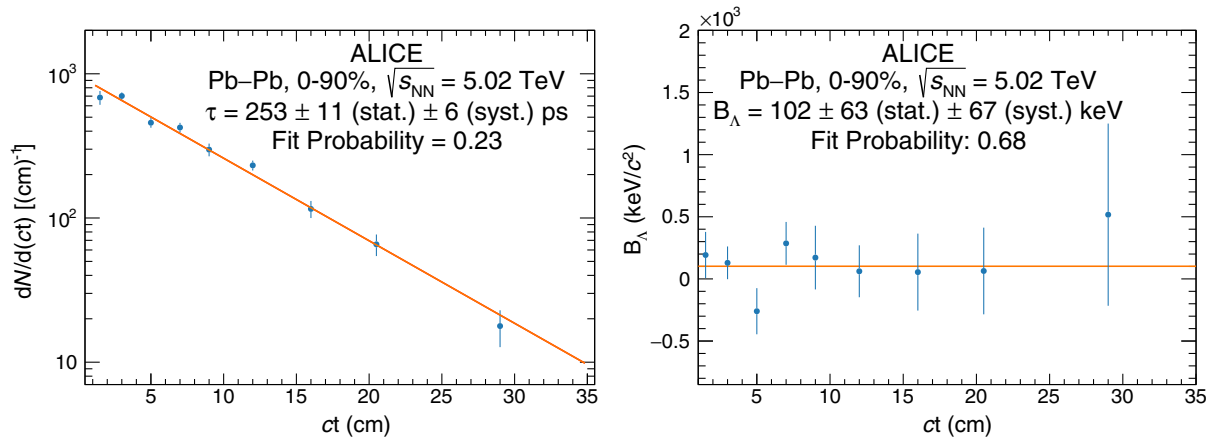


FIG. 1. Left: exponential decay spectrum as a function of the proper decay length for ${}^3_{\Lambda}\text{H}$, the blue points represent the measured yield, while the orange line represents the best fit to the measurement. Right: B_{Λ} measurement as a function of the proper decay length. Only statistical uncertainties are shown; see the text for a description of the determination of the systematic uncertainties. The fit probability computed with a Pearson test is reported.

and ${}^3_{\Lambda}\text{H}$ candidates is divided into nine $ct = ML/p$ intervals, where c is the speed of light, t is the proper time of the candidate, M is the mass of the candidate, L is the decay distance, and p is the reconstructed momentum. The BDT training and threshold optimization is repeated for each ct interval. The candidates that pass the BDT selection are used to populate the invariant-mass ($m = \sqrt{(E_{\pi} + E_{{}^3\text{He}})^2 - |\vec{p}_{\pi} + \vec{p}_{{}^3\text{He}}|^2}$) distributions, as shown in the Supplemental Material [42]. An unbinned maximum-likelihood fit is performed on the invariant-mass distribution using a kernel density estimator (KDE) function [43,44], constructed using the MC sample to describe the signal and a linear function to describe the background. The distributions obtained in the nine ct intervals can be found in the Supplemental Material [42]. The KDE is used to model the non-Gaussian behavior of the signal shape observed in the simulation by means of a superposition of Gaussian functions. The widths of the Gaussian functions are determined with an adaptive procedure that takes into account the local density of the signal in the MC sample. The yield in each ct interval is obtained from the fit to the invariant-mass spectrum. The fitted signal is corrected for the reconstruction and selection efficiency, and for the acceptance of the ALICE detector. While the interactions of the daughter particles are correctly reproduced by GEANT4 [45] and therefore naturally accounted in the efficiency determination, the interaction of the ${}^3_{\Lambda}\text{H}$ and ${}^3_{\Lambda}\bar{\text{H}}$ requires a dedicated treatment. According to Ref. [46], the expected absorption cross section of ${}^3_{\Lambda}\text{H}$ due to the inelastic interactions in the ALICE detector material is about 1.5 times that of ${}^3\bar{\text{He}}$ ($\sigma_{\text{inel}}^{{}^3\bar{\text{He}}}$). This value is used for simulating the passage of ${}^3_{\Lambda}\text{H}$ in the detector and evaluating the effect on the reconstruction efficiency. Different corrections have been applied for ${}^3_{\Lambda}\text{H}$ and ${}^3_{\Lambda}\bar{\text{H}}$ according to their expected cross sections. The typical total efficiency (including acceptance, reconstruction, and selection) is around 15% while the absorption probability of ${}^3_{\Lambda}\text{H}$ due to the inelastic interactions in the ALICE detector material is of the order of a few percent. The obtained spectrum is fitted with an exponential function as shown in the left panel of Fig. 1. The fit is performed by using the integral of the function in each bin to account for the variable widths of the ct intervals.

The major systematic uncertainties come from (1) the ${}^3_{\Lambda}\text{H}$ identification and (2) the uncertainty on the ${}^3_{\Lambda}\text{H}$ inelastic interactions in the detector. The total uncertainty is obtained as the quadratic sum of the individual contributions. The first, dominant contribution is computed by varying simultaneously the BDT selection efficiency ($\pm 10\%$), the background shape (linear, second order polynomial, and exponential), and the signal (KDE and double sided Crystal Ball [47]) fit functions in each ct interval. The systematic uncertainty is given by the rms of

the distribution of lifetimes obtained from 5×10^4 different combinations and amounts to approximately 2%. The second contribution is evaluated by varying the ${}^3_{\Lambda}\text{H}$ absorption cross section and evaluating the effect on the lifetime. The systematic uncertainty due to the assumption on the ${}^3_{\Lambda}\text{H}$ absorption cross section is evaluated by employing different cross sections for the ${}^3_{\Lambda}\text{H}$ from zero (no interaction) to $2\sigma_{\text{inel}}^{{}^3\bar{\text{He}}}$. For each variation the lifetime is recalculated, resulting in a systematic uncertainty of 1%.

The Λ separation energy B_{Λ} is obtained in each ct interval using the ${}^3_{\Lambda}\text{H}$ mass ($\mu_{{}^3_{\Lambda}\text{H}}$) extracted from the fit (see Supplemental Material [42]), the deuteron mass taken from CODATA [48], and the Λ mass taken from the PDG [49]. The reconstructed value of $\mu_{{}^3_{\Lambda}\text{H}}$ is affected by the imperfect correction for the energy loss of the daughter particles in the ALICE material. This effect produces a shift that depends on the radial distance traveled by the ${}^3_{\Lambda}\text{H}$ candidates before decaying, and it is evaluated by analyzing the MC simulations (δ_{MC}). The values of δ_{MC} as a function of the ct of the decay particles are shown in the Supplemental Material [42], and they span between -0.1 MeV and 0.8 MeV. To account for the possible mismatch between data and simulation, an additional data-driven correction is applied based on a dedicated precise measurement of the Λ mass. This represents an ideal test for the full analysis chain and for a potential data-simulation mismatch since the Λ mass is known with a precision of 6 keV [49] and its lifetime is compatible within 1σ with the ${}^3_{\Lambda}\text{H}$ one. Hence, the Λ mass is computed with the same analysis procedure employed for the ${}^3_{\Lambda}\text{H}$, and the positive shift obtained with respect to the PDG value ($\delta_{\Lambda} = 66$ keV) is used as our estimate of data-simulation mismatch and for correcting our value of $\mu_{{}^3_{\Lambda}\text{H}}$. Finally, in each ct interval B_{Λ} is computed as $B_{\Lambda} = m_d + m_{\Lambda} - (\mu_{{}^3_{\Lambda}\text{H}} - \delta_{\text{MC}} - \delta_{\Lambda})$. The final B_{Λ} value and its statistical uncertainty are obtained from the average of the values measured in each ct interval (see Fig. 1, right) weighted on their statistical uncertainties.

The systematic uncertainties on B_{Λ} originate from (1) the ${}^3_{\Lambda}\text{H}$ selection and the signal extraction, (2) the uncertainty on δ_{Λ} , and (3) the uncertainty on the ALICE material budget. The first contribution is computed using the same method as for the lifetime analysis and amounts to ± 29 keV. The uncertainty on δ_{Λ} takes into account a 60 keV shift observed by repeating the mass measurement for Λ and $\bar{\Lambda}$ with different magnetic field polarities. Finally, the systematic contribution due to the uncertainty of the ALICE material budget is computed by varying the material budget in the MC sample by its uncertainty and repeating the analysis. The B_{Λ} is recomputed for each variation, resulting in a systematic uncertainty of 8 keV. The systematic uncertainty is taken as the sum in quadrature of the three contributions. For the determination of the mean lifetime of the ${}^3_{\Lambda}\text{H}$ and its B_{Λ} , the contribution from the knowledge of the magnetic

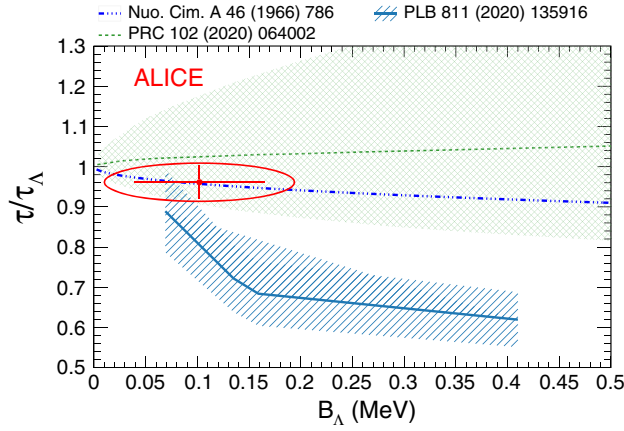


FIG. 2. The ${}^3_{\Lambda}\text{H}$ lifetime relative to the free Λ lifetime as a function of the B_{Λ} for pionless EFT [19] (green), χ EFT [20] (light blue), and the original π exchange calculations [50] (blue). The red point represents the measurement presented in this Letter with the statistical and total uncertainties depicted with lines and an ellipse, respectively.

field is considered by performing the analysis separately for positive and negative polarities of the solenoidal magnet. As the analyses with the two polarities returned results statistically compatible with each other, no further systematic uncertainty is added.

For both the lifetime and the B_{Λ} analyses, other potential sources of systematic uncertainty were tested, such as the input p_T and ct shape of ${}^3_{\Lambda}\text{H}$ in the Monte Carlo sample, the BDT hyperparameters, the discrepancy between BDT and linear selections, and the ${}^3_{\Lambda}\text{H}$ reconstruction algorithm, all resulting in a nonsignificant contribution.

The measurements for the ${}^3_{\Lambda}\text{H}$ and ${}^3_{\bar{\Lambda}}\bar{\text{H}}$ lifetime and B_{Λ} obtained with this analysis are

$$\tau = [253 \pm 11(\text{stat}) \pm 6(\text{syst})] \text{ ps},$$

$$B_{\Lambda} = [102 \pm 63(\text{stat}) \pm 67(\text{syst})] \text{ keV}.$$

As shown in Fig. 2, the measurements are in agreement with both the predictions from pionless EFT [19] and χ EFT [20], while they severely restrict the phase space available for these theories and strongly confirm the weakly bound nature of ${}^3_{\Lambda}\text{H}$. Furthermore, the new measurement of the B_{Λ} is in agreement within 1σ with the binding energy value describing best the p - Λ correlations measured with the femtoscopy technique [17,18].

Finally, the relative differences between the ${}^3_{\Lambda}\text{H}$ and ${}^3_{\bar{\Lambda}}\bar{\text{H}}$ lifetimes and masses are measured, giving the values

$$\frac{\tau_{\Lambda^3\text{H}} - \tau_{\bar{\Lambda}^3\bar{\text{H}}}}{\tau_{\Lambda^3\text{H}}} = [3 \pm 7(\text{stat}) \pm 4(\text{syst})] \times 10^{-2},$$

$$\frac{m_{\Lambda^3\text{H}} - m_{\bar{\Lambda}^3\bar{\text{H}}}}{m_{\Lambda^3\text{H}}} = [5 \pm 5(\text{stat}) \pm 3(\text{syst})] \times 10^{-5},$$

which are consistent with zero and, therefore, with the CPT symmetry expectation. Note, in the mass difference measurement, the decay daughter masses are taken to be the same between particles and antiparticles.

In summary, the most precise measurements to date of the ${}^3_{\Lambda}\text{H}$ lifetime and B_{Λ} , presented in this Letter, strongly support the loosely bound nature of ${}^3_{\Lambda}\text{H}$. The measured value perfectly agrees with the B_{Λ} that best fits the correlation

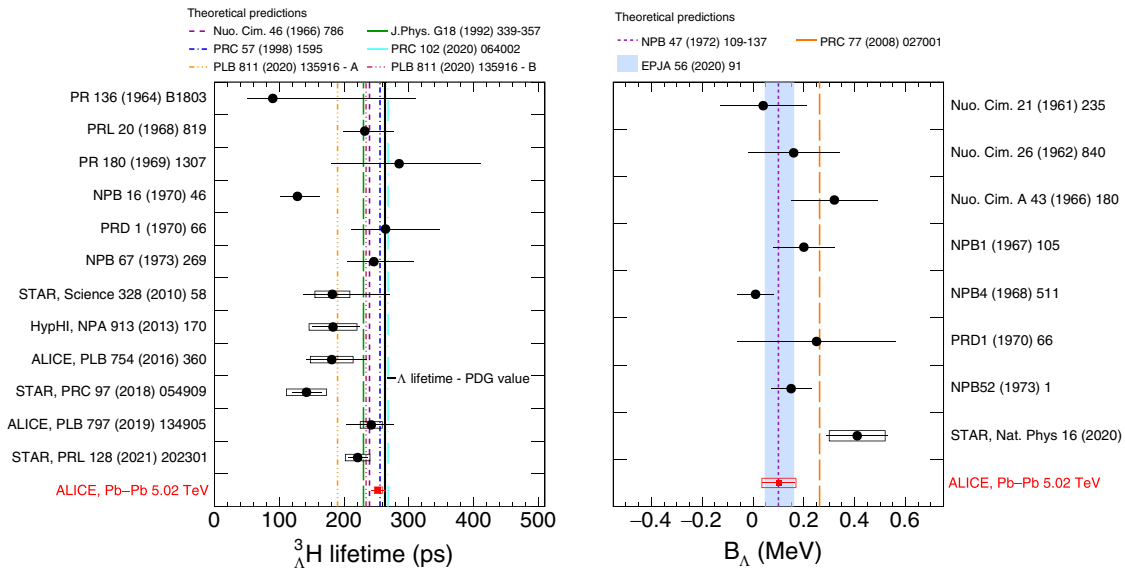


FIG. 3. Collection of the ${}^3_{\Lambda}\text{H}$ lifetime (left) [21–26,51–56] and B_{Λ} (right) [27,55,57–62] measurements obtained with different experimental techniques. The horizontal lines and boxes are the statistical and systematic uncertainties, respectively. The dashed and dash-dotted lines are the corresponding theoretical predictions [10,17,19,20,50,63–65]. Two predictions are reported in [20]: prediction A assumes $B_{\Lambda} = 130$ keV, while prediction B assumes $B_{\Lambda} = 69$ keV.

functions for protons and Λ baryons within the current theoretical approaches [16–18].

Even though some local tensions among a few measurements of lifetime and B_Λ have been reported in the literature as the “hypertriton puzzle,” when performing a global average of the historically available measurements (see Fig. 3 and the Mainz hypernuclear data database [11]), the probability of having such a set of measurements, computed with a Pearson test, is 23% for the lifetime and 57% for the B_Λ , hence no global tension is found. A remaining piece to be set for the complete understanding of the ${}^3_\Lambda\text{H}$ structure is the measurement of branching ratios for the various decay channels [19]. The Run 3 of the LHC will make those measurements accessible with unprecedented precision.

The ALICE Collaboration would like to thank all its engineers and technicians for their invaluable contributions to the construction of the experiment and the CERN accelerator teams for the outstanding performance of the LHC complex. The ALICE Collaboration gratefully acknowledges the resources and support provided by all Grid centers and the Worldwide LHC Computing Grid (WLCG) Collaboration. The ALICE Collaboration acknowledges the following funding agencies for their support in building and running the ALICE detector: A. I. Alikhanyan National Science Laboratory (Yerevan Physics Institute) Foundation (ANSL), State Committee of Science and World Federation of Scientists (WFS), Armenia; Austrian Academy of Sciences, Austrian Science Fund (FWF): [M 2467-N36] and Nationalstiftung für Forschung, Technologie und Entwicklung, Austria; Ministry of Communications and High Technologies, National Nuclear Research Center, Azerbaijan; Conselho Nacional de Desenvolvimento Científico e Tecnológico (CNPq), Financiadora de Estudos e Projetos (Finep), Fundação de Amparo à Pesquisa do Estado de São Paulo (FAPESP) and Universidade Federal do Rio Grande do Sul (UFRGS), Brazil; Bulgarian Ministry of Education and Science, within the National Roadmap for Research Infrastructures 2020–2027 (object CERN), Bulgaria; Ministry of Education of China (MOEC), Ministry of Science & Technology of China (MSTC) and National Natural Science Foundation of China (NSFC), China; Ministry of Science and Education and Croatian Science Foundation, Croatia; Centro de Aplicaciones Tecnológicas y Desarrollo Nuclear (CEADEN), Cubaenergía, Cuba; Ministry of Education, Youth and Sports of the Czech Republic, Czech Republic; The Danish Council for Independent Research—Natural Sciences, the VILLUM FONDEN and Danish National Research Foundation (DNRF), Denmark; Helsinki Institute of Physics (HIP), Finland; Commissariat à l’Énergie Atomique (CEA) and Institut National de Physique Nucléaire et de Physique des

Particules (IN2P3) and Centre National de la Recherche Scientifique (CNRS), France; Bundesministerium für Bildung und Forschung (BMBF) and GSI Helmholtzzentrum für Schwerionenforschung GmbH, Germany; General Secretariat for Research and Technology, Ministry of Education, Research and Religions, Greece; National Research, Development and Innovation Office, Hungary; Department of Atomic Energy Government of India (DAE), Department of Science and Technology, Government of India (DST), University Grants Commission, Government of India (UGC) and Council of Scientific and Industrial Research (CSIR), India; National Research and Innovation Agency—BRIN, Indonesia; Istituto Nazionale di Fisica Nucleare (INFN), Italy; Japanese Ministry of Education, Culture, Sports, Science and Technology (MEXT) and Japan Society for the Promotion of Science (JSPS) KAKENHI, Japan; Consejo Nacional de Ciencia (CONACYT) y Tecnología, through Fondo de Cooperación Internacional en Ciencia y Tecnología (FONCICYT) and Dirección General de Asuntos del Personal Académico (DGAPA), Mexico; Nederlandse Organisatie voor Wetenschappelijk Onderzoek (NWO), Netherlands; The Research Council of Norway, Norway; Commission on Science and Technology for Sustainable Development in the South (COMSATS), Pakistan; Pontificia Universidad Católica del Perú, Peru; Ministry of Education and Science, National Science Centre and WUT ID-UB, Poland; Korea Institute of Science and Technology Information and National Research Foundation of Korea (NRF), Republic of Korea; Ministry of Education and Scientific Research, Institute of Atomic Physics, Ministry of Research and Innovation and Institute of Atomic Physics and University Politehnica of Bucharest, Romania; Ministry of Education, Science, Research and Sport of the Slovak Republic, Slovakia; National Research Foundation of South Africa, South Africa; Swedish Research Council (VR) and Knut & Alice Wallenberg Foundation (KAW), Sweden; European Organization for Nuclear Research, Switzerland; Suranaree University of Technology (SUT), National Science and Technology Development Agency (NSTDA), Thailand Science Research and Innovation (TSRI) and National Science, Research and Innovation Fund (NSRF), Thailand; Turkish Energy, Nuclear and Mineral Research Agency (TENMAK), Turkey; National Academy of Sciences of Ukraine, Ukraine; Science and Technology Facilities Council (STFC), United Kingdom; National Science Foundation of the United States of America (NSF) and United States Department of Energy, Office of Nuclear Physics (DOE NP), United States of America. In addition, individual groups or members have received

support from: Marie Skłodowska Curie, European Research Council, Strong 2020—Horizon 2020 (Grants No. 950692, No. 824093, No. 896850), European Union; Academy of Finland (Center of Excellence in Quark Matter) (Grants No. 346327, No. 346328), Finland; Programa de Apoyos para la Superación del Personal Académico, UNAM, Mexico.

- [1] M. Danysz and J. Pniewski, Delayed disintegration of a heavy nuclear fragment: I, *London, Edinburgh, and Dublin Philos. Mag. J. Sci.* **44**, 348 (1953).
- [2] J. Schaffner-Bielich, *Neutron Stars* (Cambridge University Press, Cambridge, England, 2020), pp. 147–208.
- [3] J. M. Lattimer and M. Prakash, The physics of neutron stars, *Science* **304**, 536 (2004).
- [4] L. Tolos and L. Fabbietti, Strangeness in nuclei and neutron stars, *Prog. Part. Nucl. Phys.* **112**, 103770 (2020).
- [5] D. Lonardonì, A. Lovato, S. Gandolfi, and F. Pederiva, Hyperon Puzzle: Hints from Quantum Monte Carlo Calculations, *Phys. Rev. Lett.* **114**, 092301 (2015).
- [6] D. Logoteta, I. Vidana, and I. Bombaci, Impact of chiral hyperonic three-body forces on neutron stars, *Eur. Phys. J. A* **55**, 207 (2019).
- [7] L. Fabbietti, V. Mantovani Sarti, and O. Vazquez Doce, Study of the strong interaction among hadrons with correlations at the LHC, *Annu. Rev. Nucl. Part. Sci.* **71**, 377 (2021).
- [8] S. Acharya *et al.* (ALICE Collaboration), Unveiling the strong interaction among hadrons at the LHC, *Nature (London)* **588**, 232 (2020); **590**, E13 (2021).
- [9] R. H. Dalitz and G. Rajasekharan, The spins and lifetimes of the light hypernuclei, *Phys. Lett.* **1**, 58 (1962).
- [10] H. Kamada, J. Golak, K. Miyagawa, H. Witala, and W. Gloeckle, π -mesonic decay of the hypertriton, *Phys. Rev. C* **57**, 1595 (1998).
- [11] P. Eckert, P. Achenbach *et al.*, Chart of hypernuclides—Hypernuclear structure and decay data, 2021, <https://hypernuclei.kph.uni-mainz.de>.
- [12] K. Riisager, D. Fedorov, and A. Jensen, Quantum halos, *Europhys. Lett.* **49**, 547 (2000).
- [13] P. Braun-Munzinger and B. Dönigus, Loosely-bound objects produced in nuclear collisions at the LHC, *Nucl. Phys.* **A987**, 144 (2019).
- [14] A. Gal and H. Garcilazo, Towards resolving the ${}^3_{\Lambda}\text{H}$ lifetime puzzle, *Phys. Lett. B* **791**, 48 (2019).
- [15] F. Hildenbrand and H. W. Hammer, Three-body hypernuclei in pionless effective field theory, *Phys. Rev. C* **100**, 034002 (2019); **102**, 039901(E) (2020).
- [16] S. Acharya *et al.* (ALICE Collaboration), $p - p$, $p - \Lambda$, and $\Lambda - \Lambda$ correlations studied via femtoscopy in pp reactions at $\sqrt{s} = 7$ TeV, *Phys. Rev. C* **99**, 024001 (2019).
- [17] J. Haidenbauer, U. G. Meißner, and A. Nogga, Hyperon–nucleon interaction within chiral effective field theory revisited, *Eur. Phys. J. A* **56**, 91 (2020).
- [18] S. Acharya *et al.* (ALICE Collaboration), Exploring the $\text{N}\Lambda\text{-N}\Sigma$ coupled system with high precision correlation techniques at the LHC, *Phys. Lett. B* **833**, 137272 (2022).
- [19] F. Hildenbrand and H. W. Hammer, Lifetime of the hypertriton, *Phys. Rev. C* **102**, 064002 (2020).
- [20] A. Pérez-Obiol, D. Gazda, E. Friedman, and A. Gal, Revisiting the hypertriton lifetime puzzle, *Phys. Lett. B* **811**, 135916 (2020).
- [21] B. I. Abelev *et al.* (STAR Collaboration), Observation of an antimatter hypernucleus, *Science* **328**, 58 (2010).
- [22] C. Rappold *et al.*, Hypernuclear spectroscopy of products from ${}^6\text{Li}$ projectiles on a carbon target at 2 AGeV, *Nucl. Phys.* **A913**, 170 (2013).
- [23] J. Adam *et al.* (ALICE Collaboration), ${}^3_{\Lambda}\text{H}$ and ${}^3_{\Lambda}\bar{\text{H}}$ production in Pb–Pb collisions at $\sqrt{s_{\text{NN}}} = 2.76$ TeV, *Phys. Lett. B* **754**, 360 (2016).
- [24] L. Adamczyk *et al.* (STAR Collaboration), Measurement of the ${}^3_{\Lambda}\text{H}$ lifetime in Au + Au collisions at the BNL relativistic heavy ion collider, *Phys. Rev. C* **97**, 054909 (2018).
- [25] S. Acharya *et al.* (ALICE Collaboration), ${}^3_{\Lambda}\text{H}$ and ${}^3_{\Lambda}\bar{\text{H}}$ lifetime measurement in Pb–Pb collisions at $\sqrt{s_{\text{NN}}} = 5.02$ TeV via two-body decay, *Phys. Lett. B* **797**, 134905 (2019).
- [26] M. Abdallah *et al.* (STAR Collaboration), Measurements of ${}^3_{\Lambda}\text{H}$ and ${}^4_{\Lambda}\text{H}$ Lifetimes and Yields in Au + Au Collisions in the High Baryon Density Region, *Phys. Rev. Lett.* **128**, 202301 (2022).
- [27] J. Adam *et al.* (STAR Collaboration), Measurement of the mass difference and the binding energy of the hypertriton and antihypertriton, *Nat. Phys.* **16**, 409 (2020).
- [28] K. Aamodt *et al.* (ALICE Collaboration), The ALICE experiment at the CERN LHC, *J. Instrum.* **3**, S08002 (2008).
- [29] B. Abelev *et al.* (ALICE Collaboration), Performance of the ALICE experiment at the CERN LHC, *Int. J. Mod. Phys. A* **29**, 1430044 (2014).
- [30] E. Abbas *et al.* (ALICE Collaboration), Performance of the ALICE VZERO system, *J. Instrum.* **8**, P10016 (2013).
- [31] ALICE Collaboration, Centrality determination in heavy ion collisions, Report No. ALICE-PUBLIC-2018-011, 2018, <https://cds.cern.ch/record/2636623>.
- [32] K. Aamodt *et al.* (ALICE Collaboration), Alignment of the ALICE inner tracking system with cosmic-ray tracks, *J. Instrum.* **5**, P03003 (2010).
- [33] J. Alme *et al.*, The ALICE TPC, a large 3-dimensional tracking device with fast readout for ultra-high multiplicity events, *Nucl. Instrum. Methods Phys. Res., Sect. A* **622**, 316 (2010).
- [34] B. B. Abelev *et al.* (ALICE Collaboration), Production of charged pions, kaons and protons at large transverse momenta in pp and Pb–Pb collisions at $\sqrt{s_{\text{NN}}} = 2.76$ TeV, *Phys. Lett. B* **736**, 196 (2014).
- [35] S. Acharya *et al.* (ALICE Collaboration), Hypertriton Production in p–Pb Collisions at $\sqrt{s_{\text{NN}}} = 5.02$ TeV, *Phys. Rev. Lett.* **128**, 252003 (2022).
- [36] T. Chen and C. Guestrin, Xgboost: A scalable tree boosting system, in *Proceedings of the 22nd ACM SIGKDD International Conference on Knowledge Discovery and Data Mining, KDD '16* (Association for Computing Machinery, New York, NY, USA, 2016), pp. 785–794, 10.1145/2939672.2939785.
- [37] L. Barioglio, F. Catalano, M. Concas, P. Fecchio, F. Grosa, F. Mazzaschi, and M. Puccio, hipe4ml/hipe4 ml, 10.5281/zenodo.5734093 (2021).

- [38] X.-N. Wang and M. Gyulassy, HIJING: A Monte Carlo model for multiple jet production in pp, pA and AA collisions, *Phys. Rev. D* **44**, 3501 (1991).
- [39] E. Schnedermann, J. Sollfrank, and U. W. Heinz, Thermal phenomenology of hadrons from 200-A/GeV S + S collisions, *Phys. Rev. C* **48**, 2462 (1993).
- [40] S. Acharya *et al.* (ALICE Collaboration), Production of charged pions, kaons, and (anti-)protons in Pb–Pb and inelastic pp collisions at $\sqrt{s_{NN}} = 5.02$ TeV, *Phys. Rev. C* **101**, 044907 (2020).
- [41] S. Agostinelli *et al.* (GEANT4 Collaboration), GEANT4—a simulation toolkit, *Nucl. Instrum. Methods Phys. Res., Sect. A* **506**, 250 (2003).
- [42] See Supplemental Material at <http://link.aps.org/supplemental/10.1103/PhysRevLett.131.102302> for signal extraction and reconstruction shift figures.
- [43] K. S. Cranmer, Kernel estimation in high-energy physics, *Comput. Phys. Commun.* **136**, 198 (2001).
- [44] W. Verkerke and D. P. Kirkby, The RooFit toolkit for data modeling, eConf **C0303241**, MOLT007 (2003) [arXiv: physics/0306116v1].
- [45] S. Acharya *et al.* (ALICE Collaboration), First measurement of the absorption of ${}^3\text{He}$ nuclei in matter and impact on their propagation in the galaxy, *Nat. Phys.* **19**, 61 (2023).
- [46] M. V. Evlanov, A. M. Sokolov, V. K. Tartakovsky, S. A. Khorozov, and Y. Lukstins, Interaction of hypertritons with nuclei at high-energies, *Nucl. Phys.* **A632**, 624 (1998).
- [47] ALICE Collaboration, Quarkonium signal extraction in ALICE, Report No. ALICE-PUBLIC-2015-006, 2015, <https://cds.cern.ch/record/2060096>.
- [48] P. J. Mohr, D. B. Newell, and B. N. Taylor, CODATA recommended values of the fundamental physical constants: 2014, *Rev. Mod. Phys.* **88**, 035009 (2016).
- [49] P. Zyla *et al.* (Particle Data Group), Review of particle physics, *Prog. Theor. Exp. Phys.* **2020**, 083C01 (2020).
- [50] M. Rayet and R. H. Dalitz, Lifetime of ${}^3\text{H}_\Lambda$, *Nuovo Cimento Soc. Ital. Fis.* **46A**, 786 (1966).
- [51] R. J. Prem and P. H. Steinberg, Lifetimes of hypernuclei, ${}_\Lambda\text{H}^3$, ${}_\Lambda\text{H}^4$, ${}_\Lambda\text{H}^5$, *Phys. Rev.* **136**, B1803 (1964).
- [52] G. Keyes, M. Derrick, T. Fields, L. G. Hyman, J. G. Fetkovich, J. McKenzie, B. Riley, and I. T. Wang, New Measurement of the ${}_\Lambda\text{H}^3$ Lifetime, *Phys. Rev. Lett.* **20**, 819 (1968).
- [53] R. E. Phillips and J. Schneps, Lifetimes of light hyperfragments. II, *Phys. Rev.* **180**, 1307 (1969).
- [54] G. Bohm *et al.*, On the lifetime of the ${}^3_\Lambda\text{H}$ hypernucleus, *Nucl. Phys.* **B16**, 46 (1970); **B16**, 523(E) (1970).
- [55] G. Keyes, M. Derrick, T. Fields, L. G. Hyman, J. G. Fetkovich, J. Mckenzie, B. Riley, and I. T. Wang, Properties of ${}_\Lambda\text{H}^3$, *Phys. Rev. D* **1**, 66 (1970).
- [56] G. Keyes, J. Sacton, J. H. Wickens, and M. M. Block, A measurement of the lifetime of the ${}^3_\Lambda\text{H}$ hypernucleus, *Nucl. Phys.* **B67**, 269 (1973).
- [57] Y. Prakash, P. H. Steinberg, D. Chandler, and R. J. Prem, On the binding energies of mesic hypernuclei, II *Nuovo Cimento* (1955–1965) **21**, 235 (1961).
- [58] R. G. Ammar, W. Dunn, and M. Holland, On the Spin and Binding of ${}^3\text{H}_\Lambda$, *Nuovo Cim.* **26**, 840 (1962)..
- [59] C. Mayeur *et al.*, A determination of the b_λ values of light hypernuclei, II *Nuovo Cimento A* (1971–1996) **43**, 180 (1966).
- [60] W. Gajewski *et al.*, A compilation of binding energy values of light hypernuclei, *Nucl. Phys.* **B1**, 105 (1967).
- [61] G. Bohm *et al.*, A determination of the binding-energy values of light hypernuclei, *Nucl. Phys.* **B4**, 511 (1968).
- [62] M. Juric *et al.*, A new determination of the binding-energy values of the light hypernuclei ($A \leq 15$), *Nucl. Phys.* **B52**, 1 (1973).
- [63] J. G. Congleton, A simple model of the hypertriton, *J. Phys. G* **18**, 339 (1992).
- [64] R. H. Dalitz, R. C. Herndon, and Y. C. Tang, Phenomenological study of s-shell hypernuclei with ΛN and ΛNN potentials, *Nucl. Phys.* **B47**, 109 (1972).
- [65] Y. Fujiwara, Y. Suzuki, M. Kohno, and K. Miyagawa, Addendum: Triton and hypertriton binding energies calculated from SU(6) quark-model baryon-baryon interactions, *Phys. Rev. C* **77**, 027001(A) (2008).

Correction: The last sentence in the caption of Fig. 3 contained an error and has been fixed.

S. Acharya¹²⁴, D. Adamová⁸⁶, A. Adler⁶⁹, G. Aglieri Rinella³², M. Agnello²⁹, N. Agrawal⁵⁰, Z. Ahammed¹³¹, S. Ahmad¹⁵, S. U. Ahn⁷⁰, I. Ahuja³⁷, A. Akindinov¹³⁹, M. Al-Turany⁹⁷, D. Aleksandrov¹³⁹, B. Alessandro⁵⁵, H. M. Alfanda⁶, R. Alfaro Molina⁶⁶, B. Ali¹⁵, Y. Ali¹³, A. Alici²⁵, N. Alizadehvandchali¹¹³, A. Alkin³², J. Alme²⁰, G. Alocco⁵¹, T. Alt⁶³, I. Altsybeev¹³⁹, M. N. Anaam⁶, C. Andrei⁴⁵, A. Andronic¹³⁴, V. Anguelov⁹⁴, F. Antinori⁵³, P. Antonioli⁵⁰, C. Anuj¹⁵, N. Apadula⁷⁴, L. Aphecetche¹⁰³, H. Appelshäuser⁶³, C. Arata⁷³, S. Arcelli²⁵, M. Aresti⁵¹, R. Arnaldi⁵⁵, I. C. Arsene¹⁹, M. Arslanok¹³⁶, A. Augustinus³², R. Averbeck⁹⁷, M. D. Azmi¹⁵, A. Badalà⁵², Y. W. Baek⁴⁰, X. Bai¹¹⁷, R. Bailhache⁶³, Y. Bailung⁴⁷, R. Bala⁹¹, A. Balbino²⁹, A. Baldisseri¹²⁷, B. Balis², D. Banerjee⁴, Z. Banoo⁹¹, R. Barbera²⁶, F. Barile³¹, L. Barioglio⁹⁵, M. Barlou⁷⁸, G. G. Barnaföldi¹³⁵, L. S. Barnby⁸⁵, V. Barret¹²⁴, L. Barreto¹⁰⁹, C. Bartels¹¹⁶, K. Barth³², E. Bartsch⁶³, F. Baruffaldi²⁷, N. Bastid¹²⁴, S. Basu⁷⁵, G. Batigne¹⁰³, D. Battistini⁹⁵, B. Batyunya¹⁴⁰, D. Bauri⁴⁶, J. L. Bazo Alba¹⁰¹, I. G. Bearden⁸³, C. Beattie¹³⁶, P. Becht⁹⁷, D. Behera⁴⁷, I. Belikov¹²⁶, A. D. C. Bell Hechavarria¹³⁴, F. Bellini²⁵, R. Bellwied¹¹³, S. Belokurova¹³⁹, V. Belyaev¹³⁹, G. Bencedi¹³⁵

S. Beole²⁴, A. Bercuci⁴⁵, Y. Berdnikov¹³⁹, A. Berdnikova⁹⁴, L. Bergmann⁹⁴, M. G. Besoiu⁶², L. Betev³², P. P. Bhaduri¹³¹, A. Bhasin⁹¹, M. A. Bhat⁴, B. Bhattacharjee⁴¹, L. Bianchi²⁴, N. Bianchi⁴⁸, J. Bielčík³⁵, J. Bielčíková⁸⁶, J. Biernat¹⁰⁶, A. P. Bigot¹²⁶, A. Bilandzic⁹⁵, G. Biro¹³⁵, S. Biswas⁴, N. Bize¹⁰³, J. T. Blair¹⁰⁷, D. Blau¹³⁹, M. B. Blidaru⁹⁷, N. Bluhme³⁸, C. Blume⁶³, G. Boca^{21,54}, F. Bock⁸⁷, T. Bodova²⁰, A. Bogdanov¹³⁹, S. Boi²², J. Bok⁵⁷, L. Boldizsár¹³⁵, A. Bolozdynya¹³⁹, M. Bombara³⁷, P. M. Bond³², G. Bonomi^{54,130}, H. Borel¹²⁷, A. Borissov¹³⁹, A. G. Borquez Carcamo⁹⁴, H. Bossi¹³⁶, E. Botta²⁴, Y. E. M. Bouziani⁶³, L. Bratrud⁶³, P. Braun-Munzinger⁹⁷, M. Bregant¹⁰⁹, M. Broz³⁵, G. E. Bruno^{31,96}, M. D. Buckland¹¹⁶, D. Budnikov¹³⁹, H. Buesching⁶³, S. Bufalino²⁹, O. Bugnon¹⁰³, P. Buhler¹⁰², Z. Buthelezi^{67,120}, J. B. Butt¹³, S. A. Bysiak¹⁰⁶, M. Cai⁶, H. Caines¹³⁶, A. Caliva⁹⁷, E. Calvo Villar¹⁰¹, J. M. M. Camacho¹⁰⁸, P. Camerini²³, F. D. M. Canedo¹⁰⁹, M. Carabas¹²³, A. A. Carballo³², F. Carnesecchi³², R. Caron¹²⁵, J. Castillo Castellanos¹²⁷, F. Catalano^{24,29}, C. Ceballos Sanchez¹⁴⁰, I. Chakaberia⁷⁴, P. Chakraborty⁴⁶, S. Chandra¹³¹, S. Chapeland³², M. Chartier¹¹⁶, S. Chattopadhyay¹³¹, S. Chattopadhyay⁹⁹, T. G. Chavez⁴⁴, T. Cheng^{6,97}, C. Cheshkov¹²⁵, B. Cheynis¹²⁵, V. Chibante Barroso³², D. D. Chinellato¹¹⁰, E. S. Chizzali^{95,b}, J. Cho⁵⁷, S. Cho⁵⁷, P. Chochula³², P. Christakoglou⁸⁴, C. H. Christensen⁸³, P. Christiansen⁷⁵, T. Chujo¹²², M. Ciacco²⁹, C. Cicalo⁵¹, L. Cifarelli²⁵, F. Cindolo⁵⁰, M. R. Ciupek⁹⁷, G. Clai^{50,c}, F. Colamaria⁴⁹, J. S. Colburn¹⁰⁰, D. Colella^{31,96}, M. Colocci³², M. Concas^{55,d}, G. Conesa Balbastre⁷³, Z. Conesa del Valle⁷², G. Contin²³, J. G. Contreras³⁵, M. L. Coquet¹²⁷, T. M. Cormier^{87,a}, P. Cortese^{55,129}, M. R. Cosentino¹¹¹, F. Costa³², S. Costanza^{21,54}, J. Crkovská⁹⁴, P. Crochet¹²⁴, R. Cruz-Torres⁷⁴, E. Cuautle⁶⁴, P. Cui⁶, L. Cunqueiro⁸⁷, A. Dainese⁵³, M. C. Danisch⁹⁴, A. Danu⁶², P. Das⁸⁰, P. Das⁴, S. Das⁴, A. R. Dash¹³⁴, S. Dash⁴⁶, A. De Caro²⁸, G. de Cataldo⁴⁹, J. de Cuveland³⁸, A. De Falco²², D. De Gruttola²⁸, N. De Marco⁵⁵, C. De Martin²³, S. De Pasquale²⁸, S. Deb⁴⁷, R. J. Debski², K. R. Deja¹³², R. Del Grande⁹⁵, L. Dello Stritto²⁸, W. Deng⁶, P. Dhankher¹⁸, D. Di Bari³¹, A. Di Mauro³², R. A. Diaz^{7,140}, T. Dietel¹¹², Y. Ding^{6,125}, R. Divià³², D. U. Dixit¹⁸, Ø. Djuvsland²⁰, U. Dmitrieva¹³⁹, A. Dobrin⁶², B. Dönigus⁶³, A. K. Dubey¹³¹, J. M. Dubinski¹³², A. Dubla⁹⁷, S. Dudi⁹⁰, P. Dupieux¹²⁴, M. Durkac¹⁰⁵, N. Dzalaiova¹², T. M. Eder¹³⁴, R. J. Ehlers⁸⁷, V. N. Eikeland²⁰, F. Eisenhut⁶³, D. Elia⁴⁹, B. Erazmus¹⁰³, F. Ercolessi²⁵, F. Erhardt⁸⁹, M. R. Ersdal²⁰, B. Espagnon⁷², G. Eulisse³², D. Evans¹⁰⁰, S. Evdokimov¹³⁹, L. Fabbietti⁹⁵, M. Faggin²⁷, J. Faivre⁷³, F. Fan⁶, W. Fan⁷⁴, A. Fantoni⁴⁸, M. Fasel⁸⁷, P. Fedchio²⁹, A. Feliciello⁵⁵, G. Feofilov¹³⁹, A. Fernández Téllez⁴⁴, M. B. Ferrer³², A. Ferrero¹²⁷, C. Ferrero⁵⁵, A. Ferretti²⁴, V. J. G. Feuillard⁹⁴, V. Filova³⁵, D. Finogeev¹³⁹, F. M. Fionda⁵¹, F. Flor¹¹³, A. N. Flores¹⁰⁷, S. Foertsch⁶⁷, I. Fokin⁹⁴, S. Fokin¹³⁹, E. Fragiaco⁵⁶, E. Frajna¹³⁵, U. Fuchs³², N. Funicello²⁸, C. Furget⁷³, A. Furs¹³⁹, T. Fusayasu⁹⁸, J. J. Gaardhøje⁸³, M. Gagliardi²⁴, A. M. Gago¹⁰¹, C. D. Galvan¹⁰⁸, D. R. Gangadharan¹¹³, P. Ganoti⁷⁸, C. Garabatos⁹⁷, J. R. A. Garcia⁴⁴, E. Garcia-Solis⁹, K. Garg¹⁰³, C. Gargiulo³², A. Garibli⁸¹, K. Garner¹³⁴, P. Gasik⁹⁷, A. Gautam¹¹⁵, M. B. Gay Ducati⁶⁵, M. Germain¹⁰³, C. Ghosh¹³¹, S. K. Ghosh⁴, M. Giacalone²⁵, P. Giubellino^{55,97}, P. Giubilato²⁷, A. M. C. Glaenger¹²⁷, P. Glässel⁹⁴, E. Glimos¹¹⁹, D. J. Q. Goh⁷⁶, V. Gonzalez¹³³, L. H. González-Trueba⁶⁶, M. Gorgon², S. Gotovac³³, V. Grabski⁶⁶, L. K. Graczykowski¹³², E. Grecka⁸⁶, A. Grelli⁵⁸, C. Grigoras³², V. Grigoriev¹³⁹, S. Grigoryan^{1,140}, F. Grosa³², J. F. Grosse-Oetringhaus³², R. Grosso⁹⁷, D. Grund³⁵, G. G. Guardiano¹¹⁰, R. Guernane⁷³, M. Guilbaud¹⁰³, K. Gulbrandsen⁸³, T. Gundem⁶³, T. Gunji¹²¹, W. Guo⁶, A. Gupta⁹¹, R. Gupta⁹¹, S. P. Guzman⁴⁴, L. Gyulai¹³⁵, M. K. Habib⁹⁷, C. Hadjidakis⁷², H. Hamagaki⁷⁶, A. Hamdi⁷⁴, M. Hamid⁶, Y. Han¹³⁷, R. Hannigan¹⁰⁷, M. R. Haque¹³², J. W. Harris¹³⁶, A. Harton⁹, H. Hassan⁸⁷, D. Hatzifotiadou⁵⁰, P. Hauer⁴², L. B. Havener¹³⁶, S. T. Heckel⁹⁵, E. Hellbär⁹⁷, H. Helstrup³⁴, M. Hemmer⁶³, T. Herman³⁵, G. Herrera Corral⁸, F. Herrmann¹³⁴, S. Herrmann¹²⁵, K. F. Hetland³⁴, B. Heybeck⁶³, H. Hillemanns³², C. Hills¹¹⁶, B. Hippolyte¹²⁶, B. Hofman⁵⁸, B. Hohlweger⁸⁴, J. Honermann¹³⁴, G. H. Hong¹³⁷, M. Horst⁹⁵, A. Horzyk², R. Hosokawa¹⁴, Y. Hou⁶, P. Hristov³², C. Hughes¹¹⁹, P. Huhn⁶³, L. M. Huhta¹¹⁴, C. V. Hulse⁷², T. J. Humanic⁸⁸, H. Hushnud⁹⁹, A. Hutson¹¹³, D. Hutter³⁸, J. P. Iddon¹¹⁶, R. Ilkaev¹³⁹, H. Ilyas¹³, M. Inaba¹²², G. M. Innocenti³², M. Ippolitov¹³⁹, A. Isakov⁸⁶, T. Isidori¹¹⁵, M. S. Islam⁹⁹, M. Ivanov⁹⁷, M. Ivanov¹², V. Ivanov¹³⁹, V. Izucheev¹³⁹, M. Jablonski², B. Jacak⁷⁴, N. Jacazio³², P. M. Jacobs⁷⁴, S. Jadlovská¹⁰⁵, J. Jadlovsky¹⁰⁵, S. Jaelani⁸², L. Jaffe³⁸, C. Jahnke¹¹⁰, M. J. Jakubowska¹³², M. A. Janik¹³², T. Janson⁶⁹, M. Jercic⁸⁹, A. A. P. Jimenez⁶⁴, F. Jonas⁸⁷, P. G. Jones¹⁰⁰, J. M. Jowett^{32,97}, J. Jung⁶³, M. Jung⁶³, A. Junique³², A. Jusko¹⁰⁰, M. J. Kabus^{32,132}, J. Kaewjai¹⁰⁴, P. Kalinak⁵⁹, A. S. Kalteyer⁹⁷, A. Kalweit³², V. Kaplin¹³⁹, A. Karasu Uysal⁷¹, D. Karatovic⁸⁹, O. Karavichev¹³⁹

T. Karavicheva¹³⁹ P. Karczmarczyk¹³² E. Karpechev¹³⁹ V. Kashyap,⁸⁰ U. Kebschull⁶⁹ R. Keidel¹³⁸
 D. L. D. Keijndener,⁵⁸ M. Keil³² B. Ketzer⁴² A. M. Khan⁶ S. Khan¹⁵ A. Khanzadeev¹³⁹ Y. Kharlov¹³⁹
 A. Khatun¹⁵ A. Khuntia¹⁰⁶ B. Kileng³⁴ B. Kim¹⁶ C. Kim¹⁶ D. J. Kim¹¹⁴ E. J. Kim⁶⁸ J. Kim¹³⁷
 J. S. Kim⁴⁰ J. Kim⁹⁴ J. Kim⁶⁸ M. Kim^{18,94} S. Kim¹⁷ T. Kim¹³⁷ K. Kimura⁹² S. Kirsch⁶³ I. Kisel³⁸
 S. Kiselev¹³⁹ A. Kisiel¹³² J. P. Kitowski² J. L. Klay⁵ J. Klein³² S. Klein⁷⁴ C. Klein-Bösing¹³⁴
 M. Kleiner⁶³ T. Klemenz⁹⁵ A. Kluge³² A. G. Knospe¹¹³ C. Kobdaj¹⁰⁴ T. Kollegger⁹⁷ A. Kondratyev¹⁴⁰
 E. Kondratyuk¹³⁹ J. König⁶³ S. A. Konigstorfer⁹⁵ P. J. Konopka³² G. Kornakov¹³² S. D. Koryciak²
 A. Kotliarov⁸⁶ V. Kovalenko¹³⁹ M. Kowalski¹⁰⁶ V. Kozuharov³⁶ I. Králik⁵⁹ A. Kravčáková³⁷ L. Kreis,⁹⁷
 M. Krivda^{100,59} F. Krizek⁸⁶ K. Krizkova Gajdosova³⁵ M. Kroesen⁹⁴ M. Krüger⁶³ D. M. Krupova³⁵
 E. Kryshen¹³⁹ V. Kučera³² C. Kuhn¹²⁶ P. G. Kuijer⁸⁴ T. Kumaoka,¹²² D. Kumar,¹³¹ L. Kumar,⁹⁰ N. Kumar,⁹⁰
 S. Kumar³¹ S. Kundu³² P. Kurashvili⁷⁹ A. Kurepin¹³⁹ A. B. Kurepin¹³⁹ S. Kushpil⁸⁶ J. Kvapil¹⁰⁰
 M. J. Kweon⁵⁷ J. Y. Kwon⁵⁷ Y. Kwon¹³⁷ S. L. La Pointe³⁸ P. La Rocca²⁶ Y. S. Lai,⁷⁴ A. Lakrathok,¹⁰⁴
 M. Lamanna³² R. Langoy¹¹⁸ P. Larionov³² E. Laudi³² L. Lautner^{32,95} R. Lavicka¹⁰² T. Lazareva¹³⁹
 R. Lea^{54,130} G. Legras¹³⁴ J. Lehrbach³⁸ R. C. Lemmon⁸⁵ I. León Monzón¹⁰⁸ M. M. Lesch⁹⁵ E. D. Lesser¹⁸
 M. Lettrich,⁹⁵ P. Lévai¹³⁵ X. Li,¹⁰ X. L. Li,⁶ J. Lien¹¹⁸ R. Lietava¹⁰⁰ B. Lim^{16,24} S. H. Lim¹⁶ V. Lindenstruth³⁸
 A. Lindner,⁴⁵ C. Lippmann⁹⁷ A. Liu¹⁸ D. H. Liu⁶ J. Liu¹¹⁶ I. M. Lofnes²⁰ C. Loizides⁸⁷ P. Loncar³³
 J. A. Lopez⁹⁴ X. Lopez¹²⁴ E. López Torres⁷ P. Lu^{97,117} J. R. Luhder¹³⁴ M. Lunardon²⁷ G. Luparello⁵⁶
 Y. G. Ma³⁹ A. Maevskaya,¹³⁹ M. Mager³² T. Mahmoud,⁴² A. Maire¹²⁶ M. V. Makariev³⁶ M. Malaev¹³⁹
 G. Malfattore²⁵ N. M. Malik⁹¹ Q. W. Malik,¹⁹ S. K. Malik⁹¹ L. Malinina^{140,g} D. Mal'Kevich¹³⁹ D. Mallick⁸⁰
 N. Mallick⁴⁷ G. Mandaglio^{30,52} V. Manko¹³⁹ F. Manso¹²⁴ V. Manzari⁴⁹ Y. Mao⁶ G. V. Margagliotti²³
 A. Margotti⁵⁰ A. Marín⁹⁷ C. Markert¹⁰⁷ P. Martinengo³² J. L. Martinez,¹¹³ M. I. Martínez⁴⁴
 G. Martínez García¹⁰³ S. Masciocchi⁹⁷ M. Masera²⁴ A. Masoni⁵¹ L. Massacrier⁷² A. Mastroserio^{49,128}
 A. M. Mathis⁹⁵ O. Matonoha⁷⁵ P. F. T. Matuoka,¹⁰⁹ A. Matyja¹⁰⁶ C. Mayer¹⁰⁶ A. L. Mazuecos³²
 F. Mazzaschi²⁴ M. Mazzilli³² J. E. Mdhuli¹²⁰ A. F. Mechler,⁶³ Y. Melikyan¹³⁹ A. Menchaca-Rocha⁶⁶
 E. Meninno^{28,102} A. S. Menon¹¹³ M. Meres¹² S. Mhlanga,^{67,112} Y. Miake,¹²² L. Micheletti⁵⁵ L. C. Migliorin,¹²⁵
 D. L. Mihaylov⁹⁵ K. Mikhaylov^{139,140} A. N. Mishra¹³⁵ D. Miśkowiec⁹⁷ A. Modak⁴ A. P. Mohanty⁵⁸
 B. Mohanty⁸⁰ M. Mohisin Khan^{15,e} M. A. Molander⁴³ Z. Moravcova⁸³ C. Mordasini⁹⁵
 D. A. Moreira De Godoy¹³⁴ I. Morozov¹³⁹ A. Morsch³² T. Mrnjavac³² V. Muccifora⁴⁸ S. Muhuri¹³¹
 J. D. Mulligan⁷⁴ A. Mulliri,²² M. G. Munhoz¹⁰⁹ R. H. Munzer⁶³ H. Murakami¹²¹ S. Murray¹¹² L. Musa³²
 J. Musinsky⁵⁹ J. W. Myrcha¹³² B. Naik¹²⁰ A. I. Nambrath¹⁸ B. K. Nandi,⁴⁶ R. Nania⁵⁰ E. Nappi⁴⁹
 A. F. Nassirpour⁷⁵ A. Nath⁹⁴ C. Natrass¹¹⁹ M. N. Naydenov³⁶ A. Neagu,¹⁹ A. Negru,¹²³ L. Nellen⁶⁴
 S. V. Nesbo,³⁴ G. Neskovic³⁸ D. Nesterov¹³⁹ B. S. Nielsen⁸³ E. G. Nielsen⁸³ S. Nikolaev¹³⁹ S. Nikulin¹³⁹
 V. Nikulin¹³⁹ F. Noferini⁵⁰ S. Noh¹¹ P. Nomokonov¹⁴⁰ J. Norman¹¹⁶ N. Novitzky¹²² P. Nowakowski¹³²
 A. Nyanin¹³⁹ J. Nystrand²⁰ M. Ogino⁷⁶ A. Ohlson⁷⁵ V. A. Okorokov¹³⁹ J. Oleniacz¹³²
 A. C. Oliveira Da Silva¹¹⁹ M. H. Oliver¹³⁶ A. Onnerstad¹¹⁴ C. Oppedisano⁵⁵ A. Ortiz Velasquez⁶⁴
 A. Oskarsson,⁷⁵ J. Otwinowski¹⁰⁶ M. Oya,⁹² K. Oyama⁷⁶ Y. Pachmayer⁹⁴ S. Padhan⁴⁶ D. Pagano^{54,130}
 G. Paić⁶⁴ A. Palasciano⁴⁹ S. Panebianco¹²⁷ H. Park¹²² J. Park⁵⁷ J. E. Parkkila³² R. N. Patra,⁹¹ B. Paul²²
 H. Pei⁶ T. Peitzmann⁵⁸ X. Peng⁶ M. Pennisi²⁴ L. G. Pereira⁶⁵ H. Pereira Da Costa¹²⁷ D. Peresunko¹³⁹
 G. M. Perez⁷ S. Perrin¹²⁷ Y. Pestov,¹³⁹ V. Petráček³⁵ V. Petrov¹³⁹ M. Petrovici⁴⁵ R. P. Pezzi^{65,103} S. Piano⁵⁶
 M. Pikna¹² P. Pillot¹⁰³ O. Pinazza^{32,50} L. Pinsky,¹¹³ C. Pinto⁹⁵ S. Pisano⁴⁸ M. Płoskoń⁷⁴ M. Planinic,⁸⁹
 F. Pliquet,⁶³ M. G. Poghosyan⁸⁷ S. Politano²⁹ N. Poljak⁸⁹ A. Pop⁴⁵ S. Porteboeuf-Houssais¹²⁴ J. Porter⁷⁴
 V. Pozdniakov¹⁴⁰ K. K. Pradhan⁴⁷ S. K. Prasad⁴ S. Prasad⁴⁷ R. Preghenella⁵⁰ F. Prino⁵⁵ C. A. Pruneau¹³³
 I. Pshenichnov¹³⁹ M. Puccio³² S. Pucillo²⁴ Z. Pugelova,¹⁰⁵ S. Qiu⁸⁴ L. Quaglia²⁴ R. E. Quishpe,¹¹³
 S. Ragoni^{14,100} A. Rakotozafindrabe¹²⁷ L. Ramello^{55,129} F. Rami¹²⁶ S. A. R. Ramirez⁴⁴ T. A. Rancien,⁷³
 M. Rasa²⁶ S. S. Räsänen⁴³ R. Rath^{47,50} M. P. Rauch²⁰ I. Ravasenga⁸⁴ K. F. Read^{87,119} C. Reckziegel¹¹¹
 A. R. Redelbach³⁸ K. Redlich^{79,f} A. Rehman,²⁰ F. Reidt³² H. A. Reme-Ness³⁴ Z. Rescakova,³⁷ K. Reygers⁹⁴
 A. Riabov¹³⁹ V. Riabov¹³⁹ R. Ricci²⁸ T. Richert,⁷⁵ M. Richter¹⁹ A. A. Riedel⁹⁵ W. Riegler³² C. Ristea⁶²
 M. Rodríguez Cahuantzi⁴⁴ K. Røed¹⁹ R. Rogalev¹³⁹ E. Rogochaya¹⁴⁰ T. S. Rogoschinski⁶³ D. Rohr³²
 D. Röhrich²⁰ P. F. Rojas,⁴⁴ S. Rojas Torres³⁵ P. S. Rokita¹³² G. Romanenko¹⁴⁰ F. Ronchetti⁴⁸ A. Rosano^{30,52}

E. D. Rosas,⁶⁴ A. Rossi⁵³ A. Roy⁴⁷ P. Roy,⁹⁹ S. Roy,⁴⁶ N. Rubini²⁵ O. V. Rueda^{75,113} D. Ruggiano¹³² R. Rui²³
 B. Rumyantsev,¹⁴⁰ P. G. Russek² R. Russo⁸⁴ A. Rustamov⁸¹ E. Ryabinkin¹³⁹ Y. Ryabov¹³⁹ A. Rybicki¹⁰⁶
 H. Rytkonen¹¹⁴ W. Rzeska¹³² O. A. M. Saariimaki⁴³ R. Sadek¹⁰³ S. Sadhu³¹ S. Sadovsky¹³⁹ J. Saetre²⁰
 K. Šafařík³⁵ S. K. Saha⁴ S. Saha⁸⁰ B. Sahoo⁴⁶ R. Sahoo⁴⁷ S. Sahoo,⁶⁰ D. Sahu⁴⁷ P. K. Sahu⁶⁰ J. Saini¹³¹
 K. Sajdakova,³⁷ S. Sakai¹²² M. P. Salvan⁹⁷ S. Sambyal⁹¹ I. Sanna^{32,95} T. B. Saramela,¹⁰⁹ D. Sarkar¹³³
 N. Sarkar,¹³¹ P. Sarma,⁴¹ V. Sarritzu²² V. M. Sarti⁹⁵ M. H. P. Sas¹³⁶ J. Schambach⁸⁷ H. S. Scheid⁶³
 C. Schiaua⁴⁵ R. Schicker⁹⁴ A. Schmah,⁹⁴ C. Schmidt⁹⁷ H. R. Schmidt,⁹³ M. O. Schmidt³² M. Schmidt,⁹³
 N. V. Schmidt⁸⁷ A. R. Schmier¹¹⁹ R. Schotter¹²⁶ A. Schröter³⁸ J. Schukraft³² K. Schwarz,⁹⁷ K. Schweda⁹⁷
 G. Scioli²⁵ E. Scomparin⁵⁵ J. E. Seger¹⁴ Y. Sekiguchi,¹²¹ D. Sekihata¹²¹ I. Selyuzhenkov^{97,139} S. Senyukov¹²⁶
 J. J. Seo⁵⁷ D. Serebryakov¹³⁹ L. Šerkšnytė⁹⁵ A. Sevcenco⁶² T. J. Shaba⁶⁷ A. Shabetai¹⁰³ R. Shahoyan,³²
 A. Shangaraev¹³⁹ A. Sharma,⁹⁰ D. Sharma⁴⁶ H. Sharma¹⁰⁶ M. Sharma⁹¹ N. Sharma,⁹⁰ S. Sharma⁷⁶
 S. Sharma⁹¹ U. Sharma⁹¹ A. Shatat⁷² O. Sheibani,¹¹³ K. Shigaki⁹² M. Shimomura,⁷⁷ J. Shin,¹¹ S. Shirinkin¹³⁹
 Q. Shou³⁹ Y. Sibiriak¹³⁹ S. Siddhanta⁵¹ T. Siemiarzczuk⁷⁹ T. F. Silva¹⁰⁹ D. Silvermyr⁷⁵
 T. Simantathammakul,¹⁰⁴ R. Simeonov³⁶ B. Singh,⁹¹ B. Singh⁹⁵ R. Singh⁸⁰ R. Singh⁹¹ R. Singh⁴⁷ S. Singh¹⁵
 V. K. Singh¹³¹ V. Singhal¹³¹ T. Sinha⁹⁹ B. Sitar¹² M. Sitta^{55,129} T. B. Skaali,¹⁹ G. Skorodumovs⁹⁴
 M. Slupecki⁴³ N. Smirnov¹³⁶ R. J. M. Snellings⁵⁸ E. H. Solheim¹⁹ J. Song¹¹³ A. Songmoolnak,¹⁰⁴
 F. Soramel²⁷ R. Spijkers⁸⁴ I. Sputowska¹⁰⁶ J. Staa⁷⁵ J. Stachel⁹⁴ I. Stan⁶² P. J. Steffanic¹¹⁹
 S. F. Stiefelmaier⁹⁴ D. Stocco¹⁰³ I. Storehaug¹⁹ P. Stratmann¹³⁴ S. Strazzi²⁵ C. P. Stylianidis,⁸⁴
 A. A. P. Suaide¹⁰⁹ C. Suire⁷² M. Sukhanov¹³⁹ M. Suljic³² R. Sultanov¹³⁹ V. Sumberia⁹¹ S. Sumowidagdo⁸²
 S. Swain,⁶⁰ I. Szarka¹² U. Tabassam,¹³ S. F. Taghavi⁹⁵ G. Taillepied⁹⁷ J. Takahashi¹¹⁰ G. J. Tambave²⁰
 S. Tang^{6,124} Z. Tang¹¹⁷ J. D. Tapia Takaki¹¹⁵ N. Tapus,¹²³ L. A. Tarasovicova¹³⁴ M. G. Tazila⁴⁵
 G. F. Tassielli³¹ A. Tauro³² A. Telesca³² L. Terlizzi²⁴ C. Terrevoli¹¹³ G. Tersimonov,³ S. Thakur⁴
 D. Thomas¹⁰⁷ A. Tikhonov¹³⁹ A. R. Timmins¹¹³ M. Tkacik,¹⁰⁵ T. Tkacik,¹⁰⁵ A. Toia⁶³ R. Tokumoto,⁹²
 N. Topilskaya¹³⁹ M. Toppi⁴⁸ F. Torales-Acosta,¹⁸ T. Tork⁷² A. G. Torres Ramos³¹ A. Trifiró^{30,52}
 A. S. Triolo^{30,52} S. Tripathy⁵⁰ T. Tripathy⁴⁶ S. Trogolo³² V. Trubnikov³ W. H. Trzaska¹¹⁴ T. P. Trzcinski¹³²
 R. Turrisi⁵³ T. S. Tveter¹⁹ K. Ullaland²⁰ B. Ulukutlu⁹⁵ A. Uras¹²⁵ M. Urioni^{54,130} G. L. Usai²² M. Vala,³⁷
 N. Valle²¹ L. V. R. van Doremalen,⁵⁸ M. van Leeuwen⁸⁴ C. A. van Veen⁹⁴ R. J. G. van Weelden⁸⁴
 P. Vande Vyvre³² D. Varga¹³⁵ Z. Varga¹³⁵ M. Varga-Kofarago¹³⁵ M. Vasileiou⁷⁸ A. Vasiliev¹³⁹
 O. Vázquez Doce⁴⁸ V. Vechernin¹³⁹ E. Vercellin²⁴ S. Vergara Limón,⁴⁴ L. Vermunt⁹⁷ R. Vértesi¹³⁵
 M. Verweij⁵⁸ L. Vickovic,³³ Z. Vilakazi,¹²⁰ O. Villalobos Baillie¹⁰⁰ G. Vino⁴⁹ A. Vinogradov¹³⁹ T. Virgili²⁸
 V. Vislavicius,⁸³ A. Vodopyanov¹⁴⁰ B. Volkel³² M. A. Völkl⁹⁴ K. Voloshin,¹³⁹ S. A. Voloshin¹³³ G. Volpe³¹
 B. von Haller³² I. Vorobyev⁹⁵ N. Vozniuk¹³⁹ J. Vrláková³⁷ B. Wagner,²⁰ C. Wang³⁹ D. Wang,³⁹
 A. Wegrzynek³² F. T. Weiglhofer,³⁸ S. C. Wenzel³² J. P. Wessels¹³⁴ S. L. Weyhmiller¹³⁶ J. Wiechula⁶³
 J. Wikne¹⁹ G. Wilk⁷⁹ J. Wilkinson⁹⁷ G. A. Willems¹³⁴ B. Windelband,⁹⁴ M. Winn¹²⁷ J. R. Wright¹⁰⁷ W. Wu,³⁹
 Y. Wu¹¹⁷ R. Xu⁶ A. Yadav⁴² A. K. Yadav¹³¹ S. Yalcin⁷¹ Y. Yamaguchi,⁹² K. Yamakawa,⁹² S. Yang,²⁰
 S. Yano⁹² Z. Yin⁶ I.-K. Yoo¹⁶ J. H. Yoon⁵⁷ S. Yuan,²⁰ A. Yuncu⁹⁴ V. Zaccolo²³ C. Zampolli³²
 H. J. C. Zanoli,⁵⁸ F. Zanone⁹⁴ N. Zardoshti^{32,100} A. Zarochentsev¹³⁹ P. Závada⁶¹ N. Zaviyalov,¹³⁹ M. Zhalov¹³⁹
 B. Zhang⁶ L. Zhang³⁹ S. Zhang³⁹ X. Zhang⁶ Y. Zhang,¹¹⁷ Z. Zhang⁶ M. Zhao¹⁰ V. Zherebchevskii¹³⁹
 Y. Zhi,¹⁰ N. Zhigareva,¹³⁹ D. Zhou⁶ Y. Zhou⁸³ J. Zhu^{6,97} Y. Zhu,⁶ G. Zinovjev,^{3,a}
 S. C. Zugravel⁵⁵ and N. Zurlo^{130,54}

(ALICE Collaboration)

¹A.I. Alikhanyan National Science Laboratory (Yerevan Physics Institute) Foundation, Yerevan, Armenia

²AGH University of Science and Technology, Cracow, Poland

³Bogolyubov Institute for Theoretical Physics, National Academy of Sciences of Ukraine, Kiev, Ukraine

⁴Bose Institute, Department of Physics and Centre for Astroparticle Physics and Space Science (CAPSS), Kolkata, India

⁵California Polytechnic State University, San Luis Obispo, California, United States

⁶Central China Normal University, Wuhan, China

- ⁷*Centro de Aplicaciones Tecnológicas y Desarrollo Nuclear (CEADEN), Havana, Cuba*
- ⁸*Centro de Investigación y de Estudios Avanzados (CINVESTAV), Mexico City and Mérida, Mexico*
- ⁹*Chicago State University, Chicago, Illinois, United States*
- ¹⁰*China Institute of Atomic Energy, Beijing, China*
- ¹¹*Chungbuk National University, Cheongju, Republic of Korea*
- ¹²*Comenius University Bratislava, Faculty of Mathematics, Physics and Informatics, Bratislava, Slovak Republic*
- ¹³*COMSATS University Islamabad, Islamabad, Pakistan*
- ¹⁴*Creighton University, Omaha, Nebraska, United States*
- ¹⁵*Department of Physics, Aligarh Muslim University, Aligarh, India*
- ¹⁶*Department of Physics, Pusan National University, Pusan, Republic of Korea*
- ¹⁷*Department of Physics, Sejong University, Seoul, Republic of Korea*
- ¹⁸*Department of Physics, University of California, Berkeley, California, United States*
- ¹⁹*Department of Physics, University of Oslo, Oslo, Norway*
- ²⁰*Department of Physics and Technology, University of Bergen, Bergen, Norway*
- ²¹*Dipartimento di Fisica, Università di Pavia, Pavia, Italy*
- ²²*Dipartimento di Fisica dell'Università and Sezione INFN, Cagliari, Italy*
- ²³*Dipartimento di Fisica dell'Università and Sezione INFN, Trieste, Italy*
- ²⁴*Dipartimento di Fisica dell'Università and Sezione INFN, Turin, Italy*
- ²⁵*Dipartimento di Fisica e Astronomia dell'Università and Sezione INFN, Bologna, Italy*
- ²⁶*Dipartimento di Fisica e Astronomia dell'Università and Sezione INFN, Catania, Italy*
- ²⁷*Dipartimento di Fisica e Astronomia dell'Università and Sezione INFN, Padova, Italy*
- ²⁸*Dipartimento di Fisica 'E.R. Caianiello' dell'Università and Gruppo Collegato INFN, Salerno, Italy*
- ²⁹*Dipartimento DISAT del Politecnico and Sezione INFN, Turin, Italy*
- ³⁰*Dipartimento di Scienze MIFT, Università di Messina, Messina, Italy*
- ³¹*Dipartimento Interateneo di Fisica 'M. Merlin' and Sezione INFN, Bari, Italy*
- ³²*European Organization for Nuclear Research (CERN), Geneva, Switzerland*
- ³³*Faculty of Electrical Engineering, Mechanical Engineering and Naval Architecture, University of Split, Split, Croatia*
- ³⁴*Faculty of Engineering and Science, Western Norway University of Applied Sciences, Bergen, Norway*
- ³⁵*Faculty of Nuclear Sciences and Physical Engineering, Czech Technical University in Prague, Prague, Czech Republic*
- ³⁶*Faculty of Physics, Sofia University, Sofia, Bulgaria*
- ³⁷*Faculty of Science, P.J. Šafárik University, Košice, Slovak Republic*
- ³⁸*Frankfurt Institute for Advanced Studies, Johann Wolfgang Goethe-Universität Frankfurt, Frankfurt, Germany*
- ³⁹*Fudan University, Shanghai, China*
- ⁴⁰*Gangneung-Wonju National University, Gangneung, Republic of Korea*
- ⁴¹*Gauhati University, Department of Physics, Guwahati, India*
- ⁴²*Helmholtz-Institut für Strahlen- und Kernphysik, Rheinische Friedrich-Wilhelms-Universität Bonn, Bonn, Germany*
- ⁴³*Helsinki Institute of Physics (HIP), Helsinki, Finland*
- ⁴⁴*High Energy Physics Group, Universidad Autónoma de Puebla, Puebla, Mexico*
- ⁴⁵*Horia Hulubei National Institute of Physics and Nuclear Engineering, Bucharest, Romania*
- ⁴⁶*Indian Institute of Technology Bombay (IIT), Mumbai, India*
- ⁴⁷*Indian Institute of Technology Indore, Indore, India*
- ⁴⁸*INFN, Laboratori Nazionali di Frascati, Frascati, Italy*
- ⁴⁹*INFN, Sezione di Bari, Bari, Italy*
- ⁵⁰*INFN, Sezione di Bologna, Bologna, Italy*
- ⁵¹*INFN, Sezione di Cagliari, Cagliari, Italy*
- ⁵²*INFN, Sezione di Catania, Catania, Italy*
- ⁵³*INFN, Sezione di Padova, Padova, Italy*
- ⁵⁴*INFN, Sezione di Pavia, Pavia, Italy*
- ⁵⁵*INFN, Sezione di Torino, Turin, Italy*
- ⁵⁶*INFN, Sezione di Trieste, Trieste, Italy*
- ⁵⁷*Inha University, Incheon, Republic of Korea*
- ⁵⁸*Institute for Gravitational and Subatomic Physics (GRASP), Utrecht University/Nikhef, Utrecht, Netherlands*
- ⁵⁹*Institute of Experimental Physics, Slovak Academy of Sciences, Košice, Slovak Republic*
- ⁶⁰*Institute of Physics, Homi Bhabha National Institute, Bhubaneswar, India*
- ⁶¹*Institute of Physics of the Czech Academy of Sciences, Prague, Czech Republic*
- ⁶²*Institute of Space Science (ISS), Bucharest, Romania*
- ⁶³*Institut für Kernphysik, Johann Wolfgang Goethe-Universität Frankfurt, Frankfurt, Germany*
- ⁶⁴*Instituto de Ciencias Nucleares, Universidad Nacional Autónoma de México, Mexico City, Mexico*
- ⁶⁵*Instituto de Física, Universidade Federal do Rio Grande do Sul (UFRGS), Porto Alegre, Brazil*
- ⁶⁶*Instituto de Física, Universidad Nacional Autónoma de México, Mexico City, Mexico*

- ⁶⁷*iThemba LABS, National Research Foundation, Somerset West, South Africa*
- ⁶⁸*Jeonbuk National University, Jeonju, Republic of Korea*
- ⁶⁹*Johann-Wolfgang-Goethe Universität Frankfurt Institut für Informatik, Fachbereich Informatik und Mathematik, Frankfurt, Germany*
- ⁷⁰*Korea Institute of Science and Technology Information, Daejeon, Republic of Korea*
- ⁷¹*KTO Karatay University, Konya, Turkey*
- ⁷²*Laboratoire de Physique des 2 Infinis, Irène Joliot-Curie, Orsay, France*
- ⁷³*Laboratoire de Physique Subatomique et de Cosmologie, Université Grenoble-Alpes, CNRS-IN2P3, Grenoble, France*
- ⁷⁴*Lawrence Berkeley National Laboratory, California, United States*
- ⁷⁵*Lund University Department of Physics, Division of Particle Physics, Lund, Sweden*
- ⁷⁶*Nagasaki Institute of Applied Science, Nagasaki, Japan*
- ⁷⁷*Nara Women's University (NWU), Nara, Japan*
- ⁷⁸*National and Kapodistrian University of Athens, School of Science, Department of Physics, Athens, Greece*
- ⁷⁹*National Centre for Nuclear Research, Warsaw, Poland*
- ⁸⁰*National Institute of Science Education and Research, Homi Bhabha National Institute, Jatni, India*
- ⁸¹*National Nuclear Research Center, Baku, Azerbaijan*
- ⁸²*National Research and Innovation Agency - BRIN, Jakarta, Indonesia*
- ⁸³*Niels Bohr Institute, University of Copenhagen, Copenhagen, Denmark*
- ⁸⁴*Nikhef, National institute for subatomic physics, Amsterdam, Netherlands*
- ⁸⁵*Nuclear Physics Group, STFC Daresbury Laboratory, Daresbury, United Kingdom*
- ⁸⁶*Nuclear Physics Institute of the Czech Academy of Sciences, Husinec-Řež, Czech Republic*
- ⁸⁷*Oak Ridge National Laboratory, Oak Ridge, Tennessee, United States*
- ⁸⁸*Ohio State University, Columbus, Ohio, United States*
- ⁸⁹*Physics department, Faculty of science, University of Zagreb, Zagreb, Croatia*
- ⁹⁰*Physics Department, Panjab University, Chandigarh, India*
- ⁹¹*Physics Department, University of Jammu, Jammu, India*
- ⁹²*Physics Program and International Institute for Sustainability with Knotted Chiral Meta Matter (SKCM2), Hiroshima University, Hiroshima, Japan*
- ⁹³*Physikalisches Institut, Eberhard-Karls-Universität Tübingen, Tübingen, Germany*
- ⁹⁴*Physikalisches Institut, Ruprecht-Karls-Universität Heidelberg, Heidelberg, Germany*
- ⁹⁵*Physik Department, Technische Universität München, Munich, Germany*
- ⁹⁶*Politecnico di Bari and Sezione INFN, Bari, Italy*
- ⁹⁷*Research Division and ExtreMe Matter Institute EMMI, GSI Helmholtzzentrum für Schwerionenforschung GmbH, Darmstadt, Germany*
- ⁹⁸*Saga University, Saga, Japan*
- ⁹⁹*Saha Institute of Nuclear Physics, Homi Bhabha National Institute, Kolkata, India*
- ¹⁰⁰*School of Physics and Astronomy, University of Birmingham, Birmingham, United Kingdom*
- ¹⁰¹*Sección Física, Departamento de Ciencias, Pontificia Universidad Católica del Perú, Lima, Peru*
- ¹⁰²*Stefan Meyer Institut für Subatomare Physik (SMI), Vienna, Austria*
- ¹⁰³*SUBATECH, IMT Atlantique, Nantes Université, CNRS-IN2P3, Nantes, France*
- ¹⁰⁴*Suranaree University of Technology, Nakhon Ratchasima, Thailand*
- ¹⁰⁵*Technical University of Košice, Košice, Slovak Republic*
- ¹⁰⁶*The Henryk Niewodniczanski Institute of Nuclear Physics, Polish Academy of Sciences, Cracow, Poland*
- ¹⁰⁷*The University of Texas at Austin, Texas, United States*
- ¹⁰⁸*Universidad Autónoma de Sinaloa, Culiacán, Mexico*
- ¹⁰⁹*Universidade de São Paulo (USP), São Paulo, Brazil*
- ¹¹⁰*Universidade Estadual de Campinas (UNICAMP), Campinas, Brazil*
- ¹¹¹*Universidade Federal do ABC, Santo Andre, Brazil*
- ¹¹²*University of Cape Town, Cape Town, South Africa*
- ¹¹³*University of Houston, Houston, Texas, United States*
- ¹¹⁴*University of Jyväskylä, Jyväskylä, Finland*
- ¹¹⁵*University of Kansas, Lawrence, Kansas, United States*
- ¹¹⁶*University of Liverpool, Liverpool, United Kingdom*
- ¹¹⁷*University of Science and Technology of China, Hefei, China*
- ¹¹⁸*University of South-Eastern Norway, Kongsberg, Norway*
- ¹¹⁹*University of Tennessee, Knoxville, Tennessee, United States*
- ¹²⁰*University of the Witwatersrand, Johannesburg, South Africa*
- ¹²¹*University of Tokyo, Tokyo, Japan*
- ¹²²*University of Tsukuba, Tsukuba, Japan*
- ¹²³*University Politehnica of Bucharest, Bucharest, Romania*
- ¹²⁴*Université Clermont Auvergne, CNRS/IN2P3, LPC, Clermont-Ferrand, France*

¹²⁵*Université de Lyon, CNRS/IN2P3, Institut de Physique des 2 Infinis de Lyon, Lyon, France*

¹²⁶*Université de Strasbourg, CNRS, IPHC UMR 7178, F-67000 Strasbourg, France, Strasbourg, France*

¹²⁷*Université Paris-Saclay Centre d'Etudes de Saclay (CEA), IRFU, Département de Physique Nucléaire (DPnN), Saclay, France*

¹²⁸*Università degli Studi di Foggia, Foggia, Italy*

¹²⁹*Università del Piemonte Orientale, Vercelli, Italy*

¹³⁰*Università di Brescia, Brescia, Italy*

¹³¹*Variable Energy Cyclotron Centre, Homi Bhabha National Institute, Kolkata, India*

¹³²*Warsaw University of Technology, Warsaw, Poland*

¹³³*Wayne State University, Detroit, Michigan, United States*

¹³⁴*Westfälische Wilhelms-Universität Münster, Institut für Kernphysik, Munster, Germany*

¹³⁵*Wigner Research Centre for Physics, Budapest, Hungary*

¹³⁶*Yale University, New Haven, Connecticut, United States*

¹³⁷*Yonsei University, Seoul, Republic of Korea*

¹³⁸*Zentrum für Technologie und Transfer (ZTT), Worms, Germany*

¹³⁹*Affiliated with an institute covered by a cooperation agreement with CERN*

¹⁴⁰*Affiliated with an international laboratory covered by a cooperation agreement with CERN*

^aDeceased.

^bAlso at: Max-Planck-Institut für Physik, Munich, Germany.

^cAlso at: Italian National Agency for New Technologies, Energy and Sustainable Economic Development (ENEA), Bologna, Italy.

^dAlso at: Dipartimento DET del Politecnico di Torino, Turin, Italy.

^eAlso at: Department of Applied Physics, Aligarh Muslim University, Aligarh, India.

^fAlso at: Institute of Theoretical Physics, University of Wrocław, Poland.

^gAlso at: An institution covered by a cooperation agreement with CERN.